Liver X receptor activation reduces angiogenesis by impairing lipid raft localization and signaling of vascular endothelial growth factor receptor-2

Author Disclosures

Alessio Noghero: No disclosures

Alessia Perino: No disclosures

Giorgio Seano: No disclosures

Elisa Saglio: No disclosures

Giuseppe Lo Sasso: No disclosures

Franco Veglio: No disclosures

Luca Primo: No disclosures

Emilio Hirsch: No disclosures

Federico Bussolino:
Research Grant: Technological Platforms for Biotechnology (grant DRUIDI), Amount: >= $10,000
Associazione Italiana per la Ricerca sul Cancro, Amount: >= $10,000
Fondazione CRT, Amount: >= $10,000

Fulvio Morello:
Research Grant: Ricerca Sanitaria Finalizzata (Regione Piemonte), Amount: >= $10,000

Liver X Receptor activation reduces angiogenesis by impairing lipid raft localization and signaling of VEGF receptor-2

Alessio Noghero[1,2], Alessia Perino[3], Giorgio Seano[1,2], Elisa Saglio[4], Giuseppe Lo Sasso[5], Franco Veglio[6], Luca Primo[1,7], Emilio Hirsch[3], Federico Bussolino[1,2], Fulvio Morello[3,4*]

1. Institute for Cancer Research and Treatment (IRCC), Candiolo, Italy

2. Department of Oncological Sciences, University of Turin, Candiolo, Italy

3. Molecular Biotechnology Center, University of Turin, Turin, Italy

4. Emergency Department, San Giovanni Battista Hospital, Turin, Italy

5. Consorzio Mario Negri Sud, Chieti, Italy

6. Fourth Division of Internal Medicine, University of Turin, Turin, Italy

7. Department of Clinical and Biological Sciences, University of Turin, Turin, Italy

* Correspondence to Fulvio Morello, M.D., Ph.D., Emergency Department, San Giovanni Battista Hospital, C.so Bramante 88, 10126 Torino, phone +39-011-6335282 or Molecular Biotechnology Center, V. Nizza 52, 10126 Torino, Italy, phone +39-011-6706425, fax +39-011-6706432, email fulvio.morello@gmail.com

Short title	Anti-angiogenic actions of LXRs
Word count of body	5461
Word count of abstract	177
Number of Figures	6 regular, 5 supplementary

ABSTRACT

Objective - Liver X Receptors (LXRα, LXRβ) are master regulators of cholesterol homeostasis. In the endothelium, perturbations of cell cholesterol impact on fundamental processes. We therefore assessed the effects of LXR activation on endothelial functions related to angiogenesis *in vitro* and *in vivo*.

Methods and Results - LXR agonists (T0901317, GW3965) blunted migration, tubulogenesis and proliferation of human umbilical vein endothelial cells (HUVEC). By affecting endothelial cholesterol homeostasis, LXR activation impaired the compartmentation of VEGF receptor 2 (VEGFR2) in lipid rafts/caveolae and led to defective phosphorylation and downstream signaling of VEGFR2 upon VEGF-A stimulation. Consistently, the anti-angiogenic actions of LXR agonists could be prevented by co-administration of exogenous cholesterol. LXR agonists reduced endothelial sprouting from wild-type but not from LXR$\alpha^{-/-}$/LXR$\beta^{-/-}$ knock-out aortas and blunted the vascularization of implanted angioreactors *in vivo*. Furthermore, T0901317 reduced the growth of LLC-1 tumor grafts in mice by impairing angiogenesis.

Conclusions - Pharmacological activation of endothelial LXRs reduces angiogenesis by restraining cholesterol-dependent VEGFR2 compartmentation and signaling. Thus, administration of LXR agonists could exert therapeutic effects in pathological conditions characterized by uncontrolled angiogenesis.

Key words

angiogenesis, cholesterol, liver X receptor (LXR), VEGF, lipid rafts

INTRODUCTION

Liver X Receptors α and β (LXRα/NR1H3, LXRβ/NR1H2) are Retinoid X Receptor α (RXRα/ NR2B1) heterodimers belonging to the nuclear hormone receptor superfamily. Through coordinate transcriptional actions, LXRs orchestrate cellular and systemic cholesterol homeostasis.[1] LXRs reduce cholesterol absorption, inhibit cholesterol synthesis and favor cholesterol output via reverse transport and bile secretion. Endogenous LXR agonists such as 22(R)-, 24- and 25-hydroxycholesterol, are formed upon cholesterol loading of cells and mediate this physiological feedback loop.[2] Furthermore, LXR activation with synthetic agonists (e.g. T0901317, GW3965) exerts beneficial effects in atherosclerosis.[3-6]

LXRs affect cell biology well beyond cholesterol metabolism. For instance, the anti-atherosclerotic properties of LXR agonists also involve anti-inflammatory actions.[7] Moreover, LXR agonists can restrain the proliferation of several cell types by affecting cell cycle control and pro-survival pathways.[8-14] The precise mechanisms linking these complex effects to cholesterol homeostasis are largely unknown. One possibility is that LXR-dependent cholesterol mobilization may affect structure and dynamics of specific membrane and vesicular compartments. Indeed, T0901317 has been shown to reduce size and associated signaling of lipid rafts, cholesterol-enriched domains of the plasma membrane constituting fundamental signaling hubs for multiple transduction pathways.[13, 15]

Administration of LXR agonists can impair multicellular processes that involve angiogenesis, such as liver regeneration and tumor growth.[9, 13, 16] We and others have reported that endothelial cells express functional LXRs, with LXRβ representing the most important LXR isoform in this cell type.[17-19] Endothelial cells are particularly sensitive to cholesterol levels, given their wide membrane surface and richness in lipid rafts/caveolae. In line with this view, impairment of cholesterol homeostasis with itraconazole or cyclodextrin have been previously shown to affect VEGF receptor-2 (VEGFR2, Flk-1/KDR) signaling in endothelial cells.[20, 21] Taken together, these findings infer that the tissue actions of LXR agonists may also involve so far unappreciated anti-angiogenic effects.

Herein, we show that the pharmacological activation of endothelial LXRs is anti-angiogenic, as a result of synergistic reductions in cell migration, tubulogenesis and proliferation. The anti-angiogenic effects of LXR agonists involve endothelial cholesterol depletion and impaired VEGFR2

compartmentation and signaling. These findings highlight the potential for LXR-targeted therapeutic interventions in conditions of pathological angiogenesis.

METHODS

A full description of experimental methods is provided online (Supplementary Information).

Gene expression analysis

RNA was extracted using affinity columns (Qiagen) or TRIzol (Invitrogen). Microarray gene expression profiling was performed with HG-U133 Plus 2.0 microarrays (Affymetrix).[19] For quantitative reverse transcription real time-PCR (qRT-PCR), mRNA levels were analyzed using the $2^{-\Delta\Delta Ct}$ relative quantification system using 18S rRNA as housekeeping gene. Gene silencing was performed with shRNA Mission RNA interference vectors (Sigma) against LXRβ (Target Set NM_007121) or scramble shRNA.

Cell cholesterol

Lipids were extracted using chloroform:isopropanol:NP-40 (7:11:0.1). After homogenization and spinning, the organic phase was dried and suspended in a reaction mix containing cholesterol oxidase and a colorimetric probe (Biovision). Absorbance at 570 nm was finally measured in a microplate reader.

Immunofluorescence

HUVEC were fixed with 4% PFA, blocked and incubated with anti-caveolin-1 (Santacruz) and anti-VEGFR2 (R&D systems) antibodies, followed by incubation with secondary antibodies (Molecular Probes). Nuclei were counterstained with DAPI (Molecular Probes). Images were captured with a Leica AF6000 workstation equipped with a TIRF module and analyzed with ImageJ software. Tumor sections were incubated with anti-ABCA1 (Novus Biological) and/or anti-CD31 (BD Biosciences) antibodies. Images were acquired by using a Leica TCS SP2 AOBS confocal microscope and analyzed with Leica Confocal Software.

Cell fractionation

For fractionation, cell lysates were adjusted to 45% sucrose by the addition of 90% sucrose and placed into ultracentrifugation tubes. A 5-35% sucrose discontinuous gradient was formed above and samples were centrifuged at $45x10^3$ rpm for 16 hours at 4°C in a SW-55Ti rotor (Beckman). Ten fractions were collected from the top of each gradient.

Migration and tubulogenesis assays

HUVEC migration was assayed in a Boyden's chamber with a gelatin-coated polycarbonate membrane. The lower compartment of the chamber was filled with EBM-2 medium (Lonza) containing VEGF-A (10 ng/mL). HUVECs were serum-starved overnight in the presence of the indicated compounds and then added to the upper compartment of the chamber. After 5 hours of incubation, the membrane was fixed and stained for microscopic analysis.

Tubulogenesis assays were performed in solidified basement membrane matrix (Matrigel, BD Biosciences). After incubation with the indicated compounds, HUVEC were seeded and overlaid with EGM-2 medium (Lonza) containing the indicated compounds. After 8 hours, tubular structures were microscopically examined and photographed (Leica) for subsequent processing.

Cell viability and cell cycle

Cell viability was determined with the MTT assay (Roche). For apoptosis, annexin-positive HUVEC were detected using Annexin V-PE apoptosis kit (Merck). HUVEC proliferation rate and cell cycle were evaluated with the Click-iT EdU flow cytometry assay kit (Invitrogen) and propidium iodide (PI) staining, as described.[22]

Animal studies

Wild-type mice were 8-12 week-old female C57BL/6. The generation of $LXR\alpha^{-/-}/LXR\beta^{-/-}$ mice has been previously described.[23, 24] Animal procedures were approved by the local Ethical Committee.

Aortic ring angiogenic assay

Thoracic aortas were removed from 8-12 week-old mice and incubated in serum-free medium with treatment compounds.[25] Rings were transferred to Matrigel-coated culture dishes and covered with endothelial growth medium containing the indicated compounds. Tubular structures were examined with an inverted-phase contrast microscope and photographed (Leica) for subsequent processing.

In vivo neoangiogenesis

In vivo neoangiogenesis was performed using a modified Directed *In vivo* Angiogenesis Assay (DIVAA, Trevigen). On day 14, mice were euthanized and angioreactors were dissected. The vascularized basement membrane extract of each angioreactor was recovered and digested using CellSperse solution (Trevigen). Vessel-derived cells were pelleted, suspended in PBS and counted by FACS analysis.

Tumor grafts

For LLC-1 tumor grafts, 10^6 cells were injected subcutaneously into the back of 8-12 week-old female C57BL/6 mice. After one week, mice were randomized into a treatment group (T0901317 in 0.5% carboxymethyl cellulose-0.25% Tween 20, 20 mg/kg i.p. q.d.) and a control group (same amount of vehicle). Tumor growth was checked daily by caliper measurement. Mice were euthanized after one week of treatment.

Data analysis

Quantification of tubular structures was performed with WinRhizo Pro software (Regent Instruments).[26] Quantification of immunofluorescence microphotographs was performed with ImageJ software (NIH). Data are presented as average ± standard error of the mean (SEM). Statistical significance was tested with unpaired Student's *t*-test or one-way ANOVA with post-hoc analysis. The number of corresponding experimental replicates is provided in each figure legend.

RESULTS

LXR activation reduces HUVEC cholesterol

Human endothelial cells express functional LXRs.[19] Gene expression profiling by microarray (Supplementary Figure IA) and real-time PCR (Figure 1A-E) indicated that treatment of HUVEC with the synthetic LXR agonist T0901317 modulated the mRNA expression of key genes involved in cholesterol trafficking: ATP-binding cassette sub-family A member 1 (ABCA1), ATB-binding cassette sub-family G member 1 (ABCG1), inducible degrader of the low-density lipoprotein receptor (IDOL), cholesteryl ester transfer protein (CETP) and sterol regulatory element binding transcription factor 1 (SREBP1c). The up-regulation of these genes was blunted by shRNA-mediated silencing of LXRβ (Supplementary Figures IB-C and II), thus confirming that ABCA1, ABCG1, IDOL, CETP and SREBP1c are *bona fide* LXR targets also in endothelial cells.

In line with transcriptional data, T0901317 caused a robust protein induction of cholesterol transporters ABCA1 and ABCG1 (Figure 1F), which mediate cholesterol efflux and reverse cholesterol transport.[27, 28] Instead, CETP and SREBP1c protein levels were only marginally affected by T0901317 in HUVEC. Accordingly, T0901317 reduced HUVEC cholesterol content dose-dependently (Figure 1G).

LXR activation inhibits endothelial migration and tubulogenesis

Modifications in endothelial cholesterol balance and trafficking have been shown to affect key biological processes.[21, 29, 30] To assess the impact of LXR activation on endothelial angiogenesis, we first examined the effect of different LXR agonists on VEGF-A induced migration of HUVEC. LXR agonists GW3965 and T0901317 reduced migration dose-dependently compared to vehicle (Figure 2A). To rule out off-target effects of LXR-activating compounds, HUVEC migration was also evaluated in the background of LXR silencing. While T0901317 reduced the migration of HUVEC infected with scramble shRNA, T0901317 did not affect the migration of LXRβ-silenced HUVEC (Figure 2B).

HUVEC treated with GW3965 or T0901317 also showed a significant impairment in Matrigel tubulogenesis. GW3965 and T0901317 reduced average tubule length by 47±14% and 55±10% ($p<0.05$) (Figure 2C), and fork number by 63±9% and 68±11% ($p<0.05$) (Supplementary Figure IIIA)

respectively compared to vehicle. A similar effect was also produced by natural LXR agonist 22-hydroxycholesterol (Supplementary Figure IIIB). Tubulogenesis was unchanged by T0901317 when HUVEC were co-incubated with exogenous cell-soluble cholesterol, thus suggesting that LXR activation impairs *in vitro* angiogenesis by affecting cell cholesterol homeostasis (Figure 2C and Supplementary Figure IIIA). Furthermore, T0901317 reduced tubulogenesis of HUVEC infected with scramble shRNA but not with LXRβ-targeting shRNA (Figure 2D). Taken together, these findings suggested that inhibition of endothelial migration and morphogenesis by LXR agonists is mediated by LXR-specific effects on cell cholesterol homeostasis.

LXR activation inhibits endothelial proliferation without affecting apoptosis

Besides motility, angiogenesis involves endothelial proliferation. As LXR agonists have been shown to reduce cell cycle progression in non-endothelial cells,[8-11, 14] we assessed the effect of LXR agonists on HUVEC proliferation. GW3965 and T0901317 reduced HUVEC proliferation dose-dependently (Figure 3A). A similar effect was also produced by natural LXR agonist 22-hydroxycholesterol (Supplementary Figure IIIC). T0901317 reduced the protein levels of cyclins A and D1 and increased the protein levels of cyclin-dependent kinase inhibitor p27/Kip-1 (Figure 3B), indicating that LXR activation specifically perturbs cell cycle progression, as previously reported in other cell types.[14, 31, 32] However, T0901317 did not cause apoptosis (Figure 3C). Incubation of HUVEC with T0901317 specifically restrained the G_1-S cell cycle transition, as assessed by PI staining (Figure 3D), and reduced the DNA incorporation of a thymidine analogue (Figure 3E). The effect of T0901317 on G_1-S transition and DNA synthesis was relieved by co-incubation of HUVEC with exogenous cell-soluble cholesterol (Figures 3D-E), thus indicating that LXR activation impairs endothelial cell cycle and proliferation by affecting cell cholesterol homeostasis.

LXR activation reduces signaling of VEGFR2

The observed effects of LXR agonists in endothelial cells suggested the involvement of LXR in the angiogenic signaling. As previously reported in macrophages, T0901317 up-regulated the mRNA expression of VEGF-A also in HUVEC (Supplementary Figure IVA).[33] However, the protein levels of

VEGF-A were unchanged by T0901317 in HUVEC (Supplementary Figure IVB). The mRNA and protein expression of VEGFR2, the pivotal VEGF receptor controlling angiogenesis,[34] were not affected by T0901317 (Supplementary Figure IVC and Figure 4A). However, treatment of HUVEC with T0901317 blunted the functional activation of VEGFR2 by VEGF-A, as demonstrated by reduced phosphorylation of VEGFR2 on Tyr1175 and by reduced phosphorylation of phospholipase Cγ (PLCγ), a key mediator of VEGFR2-dependent angiogenic responses (Figure 4A).[34] VEGF-A-dependent phosphorylation of VEGFR2 and PLCγ was unchanged by T0901317 when HUVEC were co-incubated with exogenous cell-soluble cholesterol (Figure 4B-C), suggesting that LXR activation restrains VEGFR2 signaling by affecting cell cholesterol homeostasis. In line with this finding, the inhibitory effect of T0901317 on VEGF-A/VEGFR2-driven chemotaxis was specifically attenuated by addition of exogenous cell-soluble cholesterol (Supplementary Figures IVD). On the contrary, T0901317 treatment did not affect the migration of HUVEC stimulated by fibronectin in a haptotaxis assay (Supplementary Figure IVE).

LXR activation reduces compartmentation of VEGFR2 in lipid rafts/caveolae

Cholesterol depletion by T0901317 has been associated with a decrease in lipid raft size and signaling.[13] We thus tested the hypothesis that T0901317 may affect VEGFR2 signaling by impairing its compartmentation in lipid rafts/caveolae. We analyzed the cell surface distribution of caveolar rafts, visualized by caveolin-1 staining, and of VEGFR2, by Total Internal Reflection Fluorescence (TIRF) microscopy. Treatment of HUVEC with T0901317 reduced the caveolin-1 positive area by 53±8% ($p<0.05$) (Figures 4D-E), indicating a depletion in endothelial lipid rafts/caveolae. Furthermore, the amount of VEGFR2 localized in caveolar structures was reduced by 54±7% ($p<0.05$) (Figures 4D and 4F). The effect of T0901317 on caveolin-1 and VEGFR2 compartmentation was blunted by addition of exogenous cell-soluble cholesterol (Figures 4E-F). Membrane fractionation experiments confirmed that T0901317 displaced VEGFR2 from the buoyant flotillin-2 and caveolin-1 positive fractions (1-3), representing endothelial lipid rafts/caveolae. Instead, the amount of VEGFR2 in the heavier, binding immunoglobulin protein (BiP)-positive fractions, representing the endoplasmic reticulum, was not affected (Figures 4G-H). Co-incubation of HUVEC

with exogenous cell-soluble cholesterol attenuated the T0901317-dependent depletion of VEGFR2 in lipid rafts/caveolae (Figure 4I), indicating that LXR activation modifies VEGFR2 membrane compartmentation by affecting cell cholesterol homeostasis.

LXR activation inhibits endothelial sprouting and in vivo neoangiogenesis

The impact of LXR agonists on angiogenesis was next assayed *ex vivo* and *in vivo*. Incubation of mouse aortic rings with GW3965 or T0901317 reduced *ex vivo* endothelial sprouting by 89±2% and 73±10% respectively compared to vehicle ($p<0.05$). However, endothelial sprouting was unchanged by T0901317 when aortic rings were co-incubated with cholesterol, indicating that LXR activation impairs endothelial sprouting through cholesterol depletion (Figure 5A). T0901317 reduced endothelial sprouting when applied to aortic rings obtained from wild-type mice but not to rings obtained from mice deficient for LXRs ($LXR\alpha^{-/-}/LXR\beta^{-/-}$) (Figure 5B), thus confirming that the anti-angiogenic effect of T0901317 is LXR-specific. *In vivo* neoangiogenesis was next assessed through the subcutaneous implantation in mice of angioreactors containing VEGF-A and FGF-enriched extracellular matrix. Addition of T0901317 to the extracellular matrix critically reduced neoangiogenesis by 86±7% compared to vehicle ($p<0.05$) (Figure 5C), as assessed by red blood cell content in the angioreactors two weeks after implantation. Taken together, these data indicated that LXR agonists can inhibit angiogenesis in mouse tissues.

LXR activation inhibits tumor angiogenesis

Neoangiogenesis is strictly required for tumor growth. To highlight the effect of LXR activation on cancer angiogenesis, we used LLC-1 tumor grafts. Contrary to HUVEC, LLC-1 cells did not regulate the protein levels of cholesterol transporters ABCA1 and ABCG1 upon treatment with T0901317 (Figure 6A). Also the levels of LDLR were unchanged by T0901317 in LLC-1 cells. Of note, T0901317 did not modify the proliferation (Supplementary Figures VA-B), p27/Kip-1 expression (Supplementary Figures VC) and apoptosis (Supplementary Figures VD) of LLC-1 cells *in vitro*. LLC-1 cells were thus injected into the flank of wild-type mice, where they gave rise to palpable tumors within 7 days. Starting on day 7 post-injection, mice were treated with T0901317 or vehicle

daily (20 mg/kg i.p.) for one week. Administration of T0901317 significantly reduced tumor growth by 62±20% on day 7 compared to vehicle ($p<0.05$) (Figure 6B). Body weight remained similar in treated and control animals (data not shown). Administration of T0901317 up-regulated ABCA1 mRNA within the tumor mass (Supplementary Figure VE). In particular, T0901317 significantly increased the protein expression of ABCA1 selectively within tumor endothelial cells (Figure 6C). Of note, T0901317 treatment reduced the endothelial density of LLC-1 tumors by 50±3% compared to vehicle ($p<0.01$), as assessed by CD31 immunostaining of tumor sections (Figure 6D). Taken together, these findings indicated that pharmacological targeting of LXRs can significantly reduce tumor angiogenesis.

DISCUSSION

We provide evidence that LXR activation can restrain angiogenesis. The anti-angiogenic effects of LXR agonists are strictly connected to their impact on endothelial cholesterol homeostasis, as co-incubation of HUVEC or aortic rings with exogenous cholesterol largely neutralized the actions of LXR agonists on endothelial tubulogenesis, sprouting and proliferation. These results are in line with previous reports that drugs leading to cholesterol deprivation or to impaired cholesterol trafficking, such as β-cyclodextrin, itraconazole or high dose statins, can negatively affect angiogenesis.[29, 30, 35] In endothelial cells, T0901317 lowered cell cholesterol by regulating the expression of multiple targets. In particular, LXR activation increased the protein levels of cholesterol transporters ABCA1 and ABCG1, which promote cholesterol output towards apolipoprotein A-containing lipoproteins, as well as trans-endothelial HDL traffic.[28, 36] T0901317 also increased the mRNA expression of IDOL, which targets LDLR to ubiquitin-mediated degradation.[37] As the expression of LDLR is negligible in HUVEC, the effect of LXRs on endothelial cholesterol homeostasis is therefore essentially mediated by ABCA1 and ABCG1, at least *in vitro*. We previously reported that incubation of endothelial cells with natural LXR agonist 22(R)-hydroxycholesterol down-regulates the expression of several genes controlling cholesterol biosynthesis, such as HMG-CoA reductase, mevalonate kinase and squalene epoxidase.[19] Hence, natural oxysterol LXR ligands may further impact on endothelial cholesterol homeostasis through synergic effects on cholesterol synthesis and traffic. Nonetheless, we cannot

exclude that anti-agiogenic effects of LXRs may also relate to so far unappreciated perturbations of the non-sterol branch of the mevalonate pathway. For instance, LXR agonists may modify the synthesis of isoprenoids and affect protein prenylation, which is required for proper compartmentation and function of key proteins involved in angiogenesis (e.g. small GTPases).

Cholesterol is essential to maintain a normal structure and function of cellular membranes. Furthermore, cholesterol-rich microdomains of the plasma membrane called lipid rafts/caveolae function as preferential sites for membrane receptor clustering and signaling.[15] LXR activation has been previously shown to reduce lipid raft size and to restrain lipid-raft associated signaling in a cancer cell line.[13] We now provide evidence that in endothelial cells, treatment with LXR agonist T0901317 specifically impairs biological signals stemming from lipid raft/caveolar domains that are critical for angiogenesis. In particular, LXR activation (i) impaired VEGFR2 phosphorylation and downstream signaling to PLCγ, and (ii) blunted the compartmentation of VEGFR2 in lipid rafts/caveolae. Both effects appear to be mediated by the LXR-dependent perturbation of cholesterol homeostasis. These findings are in line with previous data showing that changes in endothelial cholesterol affect VEGFR2 signaling, most likely as a result of complex interactions of the receptor and its signaling platform within lipid rafts/caveolae.[20, 21] Nonetheless, the molecular circuitry linking cholesterol balance to angiogenesis is only beginning to emerge. In our study, LXR activation significantly reduced caveolin-rich regions of the plasma membrane. As knock-out of caveolin-1 inhibits angiogenesis by impairing VEGFR2 compartmentation and by causing a detrimental deregulation of endothelial NO synthase (eNOS), LXR activation may restrain angiogenesis by altering the physiological conditions of caveolin-1 expression and internalization, and possibly eNOS activity.[38, 39] Furthermore, as lipid rafts/caveolae are membrane microdomains harboring multiple signaling platform, we cannot exclude that the effects of LXR activation may extend to other relevant receptors and pathways such as those of FGF or TGFβ.

We provide evidence that the anti-angiogenic effects of LXR activation can be therapeutically meaningful, as T0901317 reduced both the vascularization and tumor growth of LLC-1 grafts. Of note, the anti-cancer properties of T0901317 were detectable only *in vivo*, as this drug did not modify the proliferation and apoptosis of LLC-1 cells *in vitro*. The resistance of LLC-1 cells to LXR

activation is in line with previous observations that LXR agonists can impair cell cycle progression and favor apoptosis (e.g. by increasing the expression of p27/Kip-1) only in certain cancer cell lines, while others are resistant to LXR activation.[9, 12, 13, 40]. It has been suggested that sensitivity to LXR agonists may relate to the cell-specific effects of LXRs on cholesterol homoeostasis.[31] Our findings support this hypothesis, as in LLC-1 cells T0901317 did not modify the expression of both cholesterol-handling proteins (ABCA1, ABCG1 and LDLR) and of cell cycle regulator p27/Kip-1.

Taken together, the present findings picture a scenario where LXR agonists can limit cancer growth *in vivo* by exerting substantial anti-angiogenic effects. Nonetheless, it can be foreseen that in certain cancer types, the angiostatic properties of LXR-activating compounds may synergize with direct anti-proliferative and pro-apoptotic actions of LXRs on tumor cells. As the systemic administration of LXR-activating drugs is presently limited by side effects such as liver steatosis and increased LDL-cholesterol, these drugs may find earlier applications as locally delivered therapies.

Acknowledgments

We would like to thank Dr. A. Moschetta (Consorzio Mario Negri Sud, Chieti, Italy) for kindly providing LXR$\alpha^{-/-}$/LXR$\beta^{-/-}$ mice and for precious help and discussion.

Sources of funding

This work was supported by Regione Piemonte (Ricerca Sanitaria Finalizzata 2008, 2009 to FM), Technological Platforms for Biotechnology (grant DRUIDI), AIRC and Fondazione CRT.

Disclosures

The authors have no conflicts of interest.

REFERENCES

1. Zelcer N, Tontonoz P. Liver X receptors as integrators of metabolic and inflammatory signaling. *J Clin Invest*. 2006;116(3):607-614.

2. Janowski BA, Willy PJ, Devi TR, Falck JR, Mangelsdorf DJ. An oxysterol signalling pathway mediated by the nuclear receptor LXR alpha. *Nature*. 1996;383(6602):728-731.

3. Joseph SB, McKilligin E, Pei L, Watson MA, Collins AR, Laffitte BA, Chen M, Noh G, Goodman J, Hagger GN, Tran J, Tippin TK, Wang X, Lusis AJ, Hsueh WA, Law RE, Collins JL, Willson TM, Tontonoz P. Synthetic LXR ligand inhibits the development of atherosclerosis in mice. *Proc Natl Acad Sci U S A.* 2002;99(11):7604-7609.

4. Tangirala RK, Bischoff ED, Joseph SB, Wagner BL, Walczak R, Laffitte BA, Daige CL, Thomas D, Heyman RA, Mangelsdorf DJ, Wang X, Lusis AJ, Tontonoz P, Schulman IG. Identification of macrophage liver X receptors as inhibitors of atherosclerosis. *Proc Natl Acad Sci U S A.* 2002;99(18):11896-11901.

5. Bischoff ED, Daige CL, Petrowski M, Dedman H, Pattison J, Juliano J, Li AC, Schulman IG. Non-redundant roles for LXRalpha and LXRbeta in atherosclerosis susceptibility in low density lipoprotein receptor knockout mice. *J Lipid Res.* 2010;51(5):900-906.

6. Lo Sasso G, Murzilli S, Salvatore L, D'Errico I, Petruzzelli M, Conca P, Jiang ZY, Calabresi L, Parini P, Moschetta A. Intestinal specific LXR activation stimulates reverse cholesterol transport and protects from atherosclerosis. *Cell Metab.* 2010;12(2):187-193.

7. Joseph SB, Castrillo A, Laffitte BA, Mangelsdorf DJ, Tontonoz P. Reciprocal regulation of inflammation and lipid metabolism by liver X receptors. *Nat Med.* 2003;9(2):213-219.

8. Blaschke F, Leppanen O, Takata Y, Caglayan E, Liu J, Fishbein MC, Kappert K, Nakayama KI, Collins AR, Fleck E, Hsueh WA, Law RE, Bruemmer D. Liver X Receptor Agonists Suppress Vascular Smooth Muscle Cell Proliferation and Inhibit Neointima Formation in Balloon-Injured Rat Carotid Arteries. *Circ Res.* 2004;95(12):e110-123.

9. Fukuchi J, Kokontis JM, Hiipakka RA, Chuu C-p, Liao S. Antiproliferative Effect of Liver X Receptor Agonists on LNCaP Human Prostate Cancer Cells. *Cancer Res.* 2004;64(21):7686-7689.

10. Wente W, Brenner MB, Zitzer H, Gromada J, Efanov AM. Activation of Liver X Receptors and Retinoid X Receptors Induces Growth Arrest and Apoptosis in Insulin-Secreting Cells. *Endocrinology*. 2007;148(4):1843-1849.

11. Meng Z, Nie J, Ling J, Sun J, Zhu Y, Gao L, Lv J, Zhu D, Sun Y, Han X. Activation of liver X receptors inhibits pancreatic islet beta cell proliferation through cell cycle arrest. *Diabetologia.* 2009;52(1):125-135.

12. Chuu C-P, Lin H-P. Antiproliferative Effect of LXR Agonists T0901317 and 22(R)-Hydroxycholesterol on Multiple Human Cancer Cell Lines. *Anticancer Res.* 2010;30(9):3643-3648.

13. Pommier AJ, Alves G, Viennois E, Bernard S, Communal Y, Sion B, Marceau G, Damon C, Mouzat K, Caira F, Baron S, Lobaccaro JM. Liver X Receptor activation downregulates AKT survival signaling in lipid rafts and induces apoptosis of prostate cancer cells. *Oncogene.* 2010;29(18):2712-2723.

14. Bensinger SJ, Bradley MN, Joseph SB, Zelcer N, Janssen EM, Hausner MA, Shih R, Parks JS, Edwards PA, Jamieson BD, Tontonoz P. LXR signaling couples sterol metabolism to proliferation in the acquired immune response. *Cell.* 2008;134(1):97-111.

15. Lingwood D, Simons K. Lipid rafts as a membrane-organizing principle. *Science.* 2010;327(5961):46-50.

16. Lo Sasso G, Celli N, Caboni M, Murzilli S, Salvatore L, Morgano A, Vacca M, Pagliani T, Parini P, Moschetta A. Down-regulation of the LXR transcriptome provides the requisite cholesterol levels to proliferating hepatocytes. *Hepatology.* 2009;51(4):1334-1344.

17. Liao H, Langmann T, Schmitz G, Zhu Y. Native LDL Upregulation of ATP-Binding Cassette Transporter-1 in Human Vascular Endothelial Cells. *Arterioscler Thromb Vasc Biol.* 2002;22(1):127-132.

18. Norata GD, Ongari M, Uboldi P, Pellegatta F, Catapano AL. Liver X receptor and retinoic X receptor agonists modulate the expression of genes involved in lipid metabolism in human endothelial cells. *Int J Mol Med.* 2005;16(4):717-722.

19. Morello F, Saglio E, Noghero A, Schiavone D, Williams TA, Verhovez A, Bussolino F, Veglio F, Mulatero P. LXR-activating oxysterols induce the expression of inflammatory markers in endothelial cells through LXR-independent mechanisms. *Atherosclerosis.* 2009;207(1):38-44.

20. Labrecque L, Royal I, Surprenant DS, Patterson C, Gingras D, Beliveau R. Regulation of vascular endothelial growth factor receptor-2 activity by caveolin-1 and plasma membrane cholesterol. *Mol Biol Cell.* 2003;14(1):334-347.

21. Liao W-X, Feng L, Zhang H, Zheng J, Moore TR, Chen D-B. Compartmentalizing VEGF-Induced ERK2/1 Signaling in Placental Artery Endothelial Cell Caveolae: A Paradoxical Role of Caveolin-1 in Placental Angiogenesis in Vitro. *Mol Endocrinol.* 2009;23(9):1428-1444.

22. Noghero A, Arese M, Bussolino F, Gualandris A. Mature endothelium and neurons are simultaneously derived from embryonic stem cells by 2D in vitro culture system. *J Cell Mol Med.* 2011;15(10):2200-2215.

23. Peet DJ, Turley SD, Ma W, Janowski BA, Lobaccaro J-MA, Hammer RE, Mangelsdorf DJ. Cholesterol and Bile Acid Metabolism Are Impaired in Mice Lacking the Nuclear Oxysterol Receptor LXR[alpha]. *Cell.* 1998;93(5):693-704.

24. Repa JJ, Turley SD, Lobaccaro J-MA, Medina J, Li L, Lustig K, Shan B, Heyman RA, Dietschy JM, Mangelsdorf DJ. Regulation of Absorption and ABC1-Mediated Efflux of Cholesterol by RXR Heterodimers. *Science.* 2000;289(5484):1524-1529.

25. Primo L, Seano G, Roca C, Maione F, Gagliardi PA, Sessa R, Martinelli M, Giraudo E, di Blasio L, Bussolino F. Increased Expression of alpha6 Integrin in Endothelial Cells Unveils a Proangiogenic Role for Basement Membrane. *Cancer Res.* 2010;70(14):5759-5769.

26. Cascone I, Napione L, Maniero F, Serini G, Bussolino F. Stable interaction between alpha5beta1 integrin and Tie2 tyrosine kinase receptor regulates endothelial cell response to Ang-1. *J Cell Biol.* 2005;170(6):993-1004.

27. Vaisman BL, Demosky SJ, Stonik JA, Ghias M, Knapper CL, Sampson ML, Dai C, Levine SJ, Remaley AT. Endothelial expression of human ABCA1 in mice increases plasma HDL cholesterol and reduces diet-induced atherosclerosis. *J Lipid Res.* 2012;53(1):158-167.

28. Rohrer L, Ohnsorg PM, Lehner M, Landolt F, Rinninger F, von Eckardstein A. High-Density Lipoprotein Transport Through Aortic Endothelial Cells Involves Scavenger Receptor BI and ATP-Binding Cassette Transporter G1. *Circ Res.* 2009;104(10):1142-1150.

29. Xu J, Dang Y, Ren YR, Liu JO. Cholesterol trafficking is required for mTOR activation in endothelial cells. *Proc Natl Acad Sci U S A.* 2010;107(10):4764-4769.

30. Vincent L, Chen W, Hong L, Mirshahi F, Mishal Z, Mirshahi-Khorassani T, Vannier J-P, Soria J, Soria C. Inhibition of endothelial cell migration by cerivastatin, an HMG-CoA reductase inhibitor: contribution to its anti-angiogenic effect. *FEBS Letters.* 2001;495(3):159-166.

31. Kim KH, Lee GY, Kim JI, Ham M, Won Lee J, Kim JB. Inhibitory effect of LXR activation on cell proliferation and cell cycle progression through lipogenic activity. *J Lipid Res.* 2010;51(12):3425-3433.

32. Vedin LL, Lewandowski SA, Parini P, Gustafsson JA, Steffensen KR. The oxysterol receptor LXR inhibits proliferation of human breast cancer cells. *Carcinogenesis.* 2009;30(4):575-579.

33. Walczak R, Joseph SB, Laffitte BA, Castrillo A, Pei L, Tontonoz P. Transcription of the vascular endothelial growth factor gene in macrophages is regulated by liver X receptors. *J Biol Chem.* 2004;279(11):9905-9911.

34. Olsson A-K, Dimberg A, Kreuger J, Claesson-Welsh L. VEGF receptor signalling - in control of vascular function. *Nat Rev Mol Cell Biol.* 2006;7(5):359-371.

35. Vincent Lc, Soria C, Mirshahi F, Opolon P, Mishal Z, Vannier J-P, Soria J, Hong L. Cerivastatin, an Inhibitor of 3-Hydroxy-3-Methylglutaryl Coenzyme A Reductase, Inhibits Endothelial Cell Proliferation Induced by Angiogenic Factors In Vitro and Angiogenesis in In Vivo Models. *Arterioscler Thromb Vasc Biol.* 2002;22(4):623-629.

36. Panzenboeck U, Balazs Z, Sovic A, Hrzenjak A, Levak-Frank S, Wintersperger A, Malle E, Sattler W. ABCA1 and Scavenger Receptor Class B, Type I, Are Modulators of Reverse Sterol Transport at an in Vitro Blood-Brain Barrier Constituted of Porcine Brain Capillary Endothelial Cells. *J Biol Chem.* 2002;277(45):42781-42789.

37. Zelcer N, Hong C, Boyadjian R, Tontonoz P. LXR Regulates Cholesterol Uptake Through Idol-Dependent Ubiquitination of the LDL Receptor. *Science.* 2009;325(5936):100-104.

38. Sonveaux P, Martinive P, DeWever J, Batova Z, Daneau Gr, Pelat M, Ghisdal P, Grégoire V, Dessy C, Balligand J-L, Feron O. Caveolin-1 Expression Is Critical for Vascular Endothelial Growth

Factor-Induced Ischemic Hindlimb Collateralization and Nitric Oxide-Mediated Angiogenesis. *Circ Res.* 2004;95(2):154-161.

39. Morais C, Ebrahem Q, Anand-Apte B, Parat M-O. Altered Angiogenesis in Caveolin-1 Gene-Deficient Mice Is Restored by Ablation of Endothelial Nitric Oxide Synthase. *Am J Pathol.* 2012;180(4):1702-1714.

40. Mehrotra A, Kaul D, Joshi K. LXR-α selectively reprogrammes cancer cells to enter into apoptosis. *Mol Cell Biochem*. 2011;349(1):41-55.

FIGURE LEGENDS

Figure 1. LXR activation reduces endothelial cholesterol. (**A**-**E**) Relative mRNA expression of LXR target genes ABCA1, ABCG1, IDOL, CETP, SREBP1c in HUVEC treated for 18 hours with T0901317 (T090, 1 μM) or vehicle (DMSO). *p<0.05, ***p<0.001, n=4. (**F**) Protein levels of ABCA1, ABCG1, CETP, SREBP1c (p=precursor, m=mature) in HUVEC treated for 18 hours with T0901317 (1 μM) or vehicle (DMSO). Representative blot of 3 experiments. (**G**) Cell cholesterol (pg/cell) in HUVEC treated for 24 hours with T0901317 (1, 10 μM) or vehicle (DMSO). **p<0.01, ***p<0.001 versus DMSO, n=4.

Figure 2. LXR activation impairs endothelial migration and tubulogenesis. (**A**) VEGF-A-induced migration of HUVEC treated for 18 hours with GW3965 (1 or 10 μM), T0901317 (T090, 1 or 10 μM) or vehicle (DMSO). **p<0.01, ***p<0.001 versus DMSO, n=4. (**B**) VEGF-A-induced migration of LXRβ-silenced (shRNA-LXRβ_2/3) or control HUVEC (shRNA scramble) treated for 18 hours with T0901317 (10 μM) or vehicle (DMSO). **p<0.01 versus DMSO, n=4. (**C**) Matrigel tubulogenesis of HUVEC treated for 18 hours with the indicated compounds: vehicle (DMSO), cholesterol (CHOL, 20 μM), GW3965 (10 μM) or T0901317 (10 μM). Left: representative images of endothelial tubules. Right: quantification of relative tubule length per digital image, expressed as % of control (DMSO). *p<0.05 versus DMSO, †p<0.05 versus T090+CHOL, n=4. (**D**) Matrigel tubulogenesis of LXRβ-silenced (shRNA-LXRβ_2/3) or control HUVEC (shRNA scramble) treated as in B. Left:

representative images of endothelial tubules. Right: quantification of relative tubule length per digital image, expressed as % of DMSO-treated shRNA scramble. **p<0.01 versus DMSO, n=4.

Figure 3. LXR activation impairs endothelial proliferation without affecting apoptosis. (**A**) Cell growth of HUVEC treated for 48 hours with vehicle (DMSO), GW3965 (1, 5, 10 μM) or T0901317 (T090, 1, 5, 10 μM). Cell growth was assessed by MTT. ***p<0.001 versus DMSO, n=6. (**B**) Protein levels of cyclin A, cyclin D1 and p27/Kip-1 in HUVEC treated for 24 hours with DMSO or T0901317 (10 μM). Representative blots of 3 experiments. (**C**) Apoptosis of HUVEC treated for 24 hours with the indicated compounds: vehicle (DMSO), GW3965 (10 μM), T0901317 (10 μM). starve: EBM-2 medium, GM: EGM-2 medium. ***p<0.01 versus DMSO, n=6. (**D**) Cell cycle distribution of HUVEC treated for 24 hours with vehicle (DMSO), cholesterol (CHOL, 20 μM), T0901317 (10 μM). DNA content was determined by PI staining and assessed by FACS analysis (representative experiment, n=3). (**E**) Proliferation rate of HUVEC treated as in D. DNA incorporation of the thymidine fluorescent analogue EdU was detected by flow cytometry. The % of proliferating cells is indicated (representative experiment, n=3).

Figure 4. LXR activation impairs VEGFR2 signaling and compartmentation in lipid rafts/caveolae. (**A**) Protein levels of phospho-VEGFR2, total VEGFR2 and phospho-PLCγ in HUVEC treated with VEGF-A (30 ng/mL, 5 minutes) after incubation for 18 hours with vehicle (DMSO), T0901317 (T090, 10 μM), cholesterol (CHOL, 20 μM). Representative blots of 4 experiments. (**B**) Quantification of P-VEGFR2 in HUVEC treated as in A. ***p<0.001 versus DMSO, †p<0.05 versus T090+CHOL, n=4. (**C**) Quantification of P-PLCγ in HUVEC treated as in A. ***p<0.001 versus DMSO, ††p<0.01 versus T090+CHOL, n=3. (**D**) Immunofluorescence staining of HUVEC treated for 18 hours with vehicle (DMSO), T0901317 (10 μM), cholesterol (20 μM). Representative images of Total Internal Reflection Fluorescence (TIRF): red (caveolin-1), green (VEGRF2), blue (DAPI), yellow (merge caveolin-1/VEGFR2). (**E**) Quantification of cell surface caveolin-1-positive area. *p<0.05 versus DMSO, †††p<0.001 versus T090+CHOL, n=20. (**F**) Quantification of cell surface VEGFR2 in caveolin-1-positive areas. **p<0.01 versus DMSO, †††p<0.001 versus T090+CHOL,

n=20. (**G-I**) Distribution of VEGFR2, flotillin-2 (Flot-2), caveolin-1 (Cav-1) and binding immunoglobulin protein (BiP) in the protein fractions obtained from HUVEC (ultracentrifugation on a discontinuous sucrose gradient) treated as in D. The lipid raft compartment is represented in the lighter fractions (1-3), while the endoplasmic reticulum peaks in the heavier fractions (7-10). Representative blots of 3 experiments.

Figure 5. LXR activation impairs angiogenesis in mouse tissues. (**A**) Endothelial sprouting from mouse aortic rings incubated with the indicated compounds for 5 days: vehicle (DMSO), GW3965 (10 μM), T0901317 (T090, 10 μM), cholesterol (CHOL, 20 μM). Left: representative images of sprouting. *p<0.05 versus DMSO, †p<0.05 versus T090+CHOL, n=4. (**B**) Endothelial sprouting from wild-type (WT) and LXRα$^{-/-}$/LXRβ$^{-/-}$ (LXR-DOKO) aortic rings incubated with vehicle (DMSO) or T0901317 (10 μM). **p<0.01 versus DMSO, n=4. (**C**) Neoangiogenesis in angioreactors implanted subcutaneously in wild-type mice for two weeks. Left: representative images of explanted angioreactors filled with basement membrane extract containing VEGF-A and FGF-2 plus vehicle (DMSO) or T0901317 (10 μM). ***p<0.001, n=14.

Figure 6. LXR activation reduces tumor angiogenesis. (**A**) Protein levels of ABCA1, ABCG1, LDLR in HUVEC and LLC-1 cells treated for 18 hours with vehicle (DMSO) or T0901317 (T090, 1 μM). Representative blots of 3 experiments. (**B**) Growth curve of LLC-1 tumor grafts in mice treated with vehicle (CMC-Tween 20) or T0901317 (20 mg/kg i.p. q.d.) for one week. Tumor volume was calculated based on daily caliper measurements. *p<0.05, **p<0.01, n=10 mice per group. (**C**) ABCA1/CD31 immunostaining in tumor vessels. Treatments were performed as in B. Left: representative images (red: ABCA1, green: CD31, blue: DAPI), 40x magnification, scale bar 30 μm. Right: quantification of ABCA1 fluorescence in CD31+ areas. **p<0.01, n=10 per group. (**D**) CD31 immunostaining in tumor sections. Treatments were performed as in B. Left: representative images, 10x magnification, scale bar 100 μm (green: CD31, blue: DAPI). Right: quantification of CD31 immunofluorescence (% of tumor area). **p<0.01, n=10 per group.

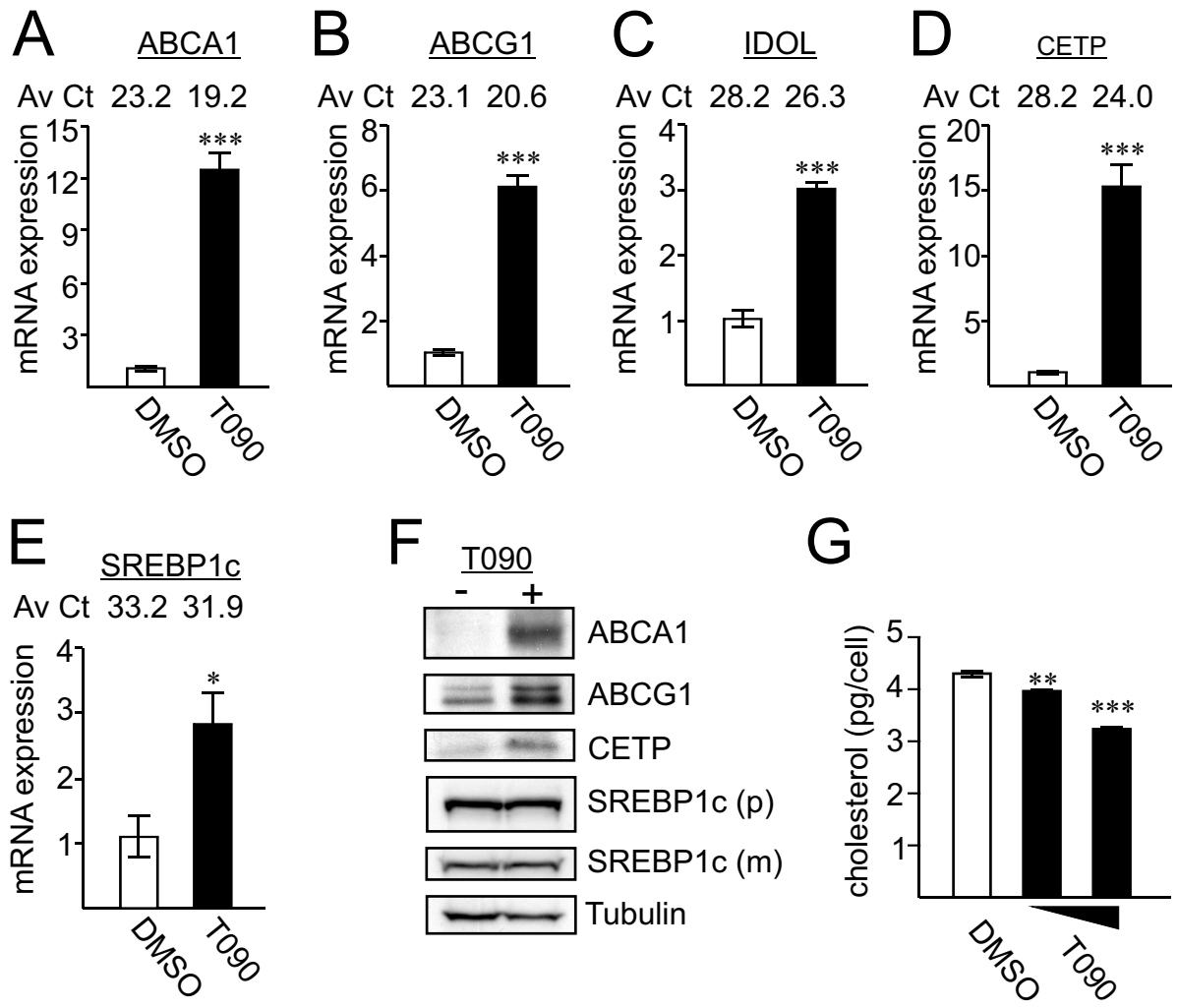

Figure 1

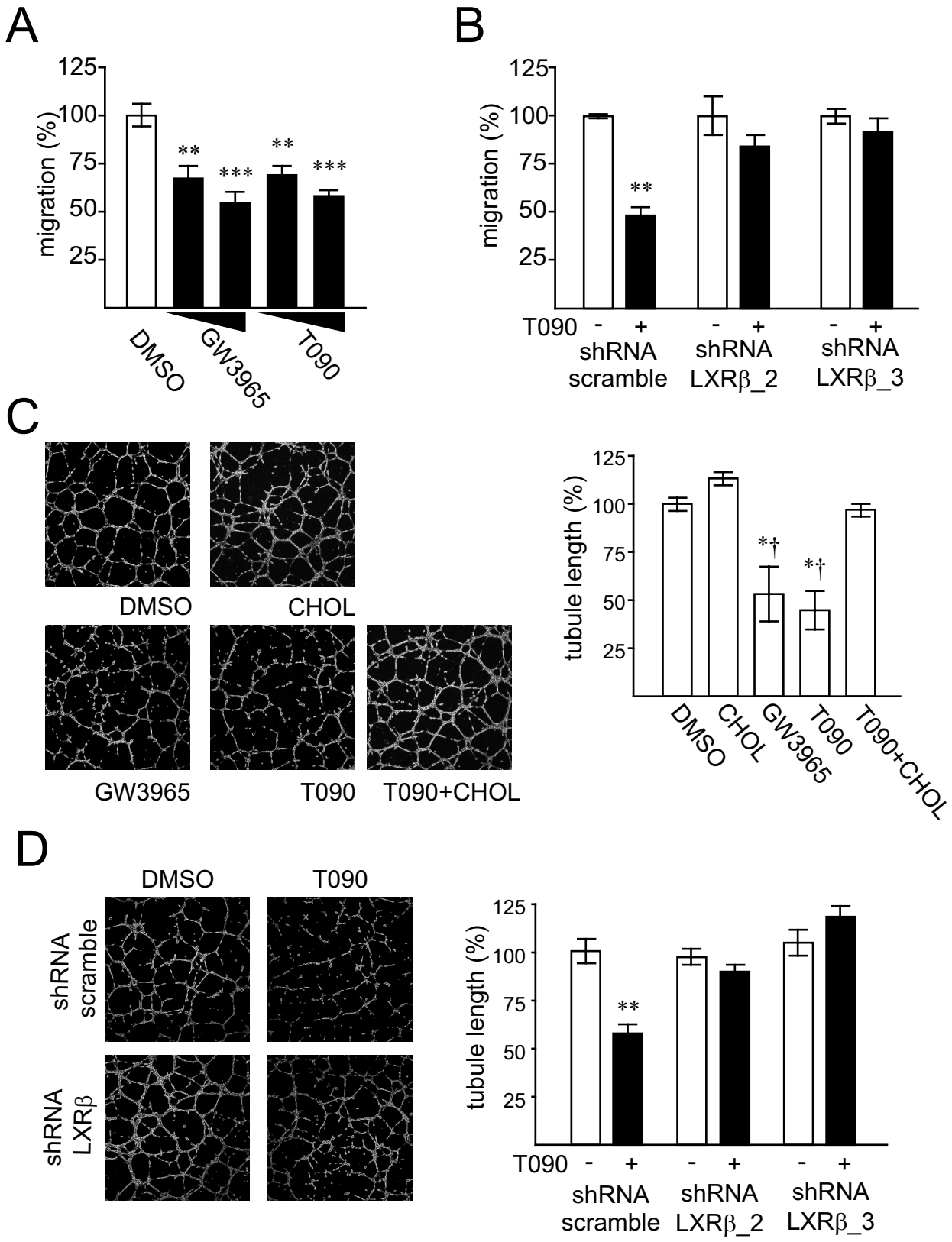

Figure 2

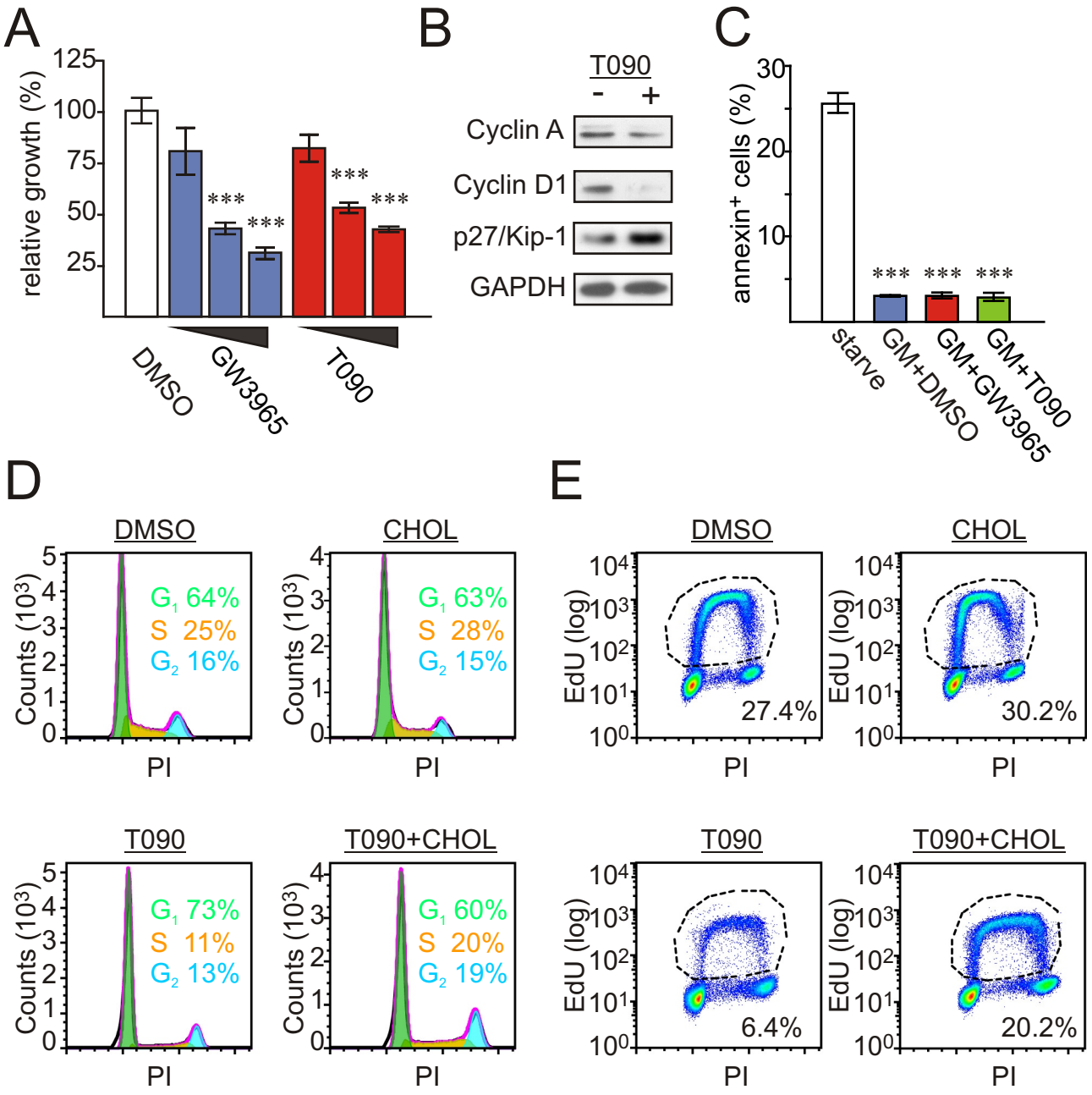

Figure 3

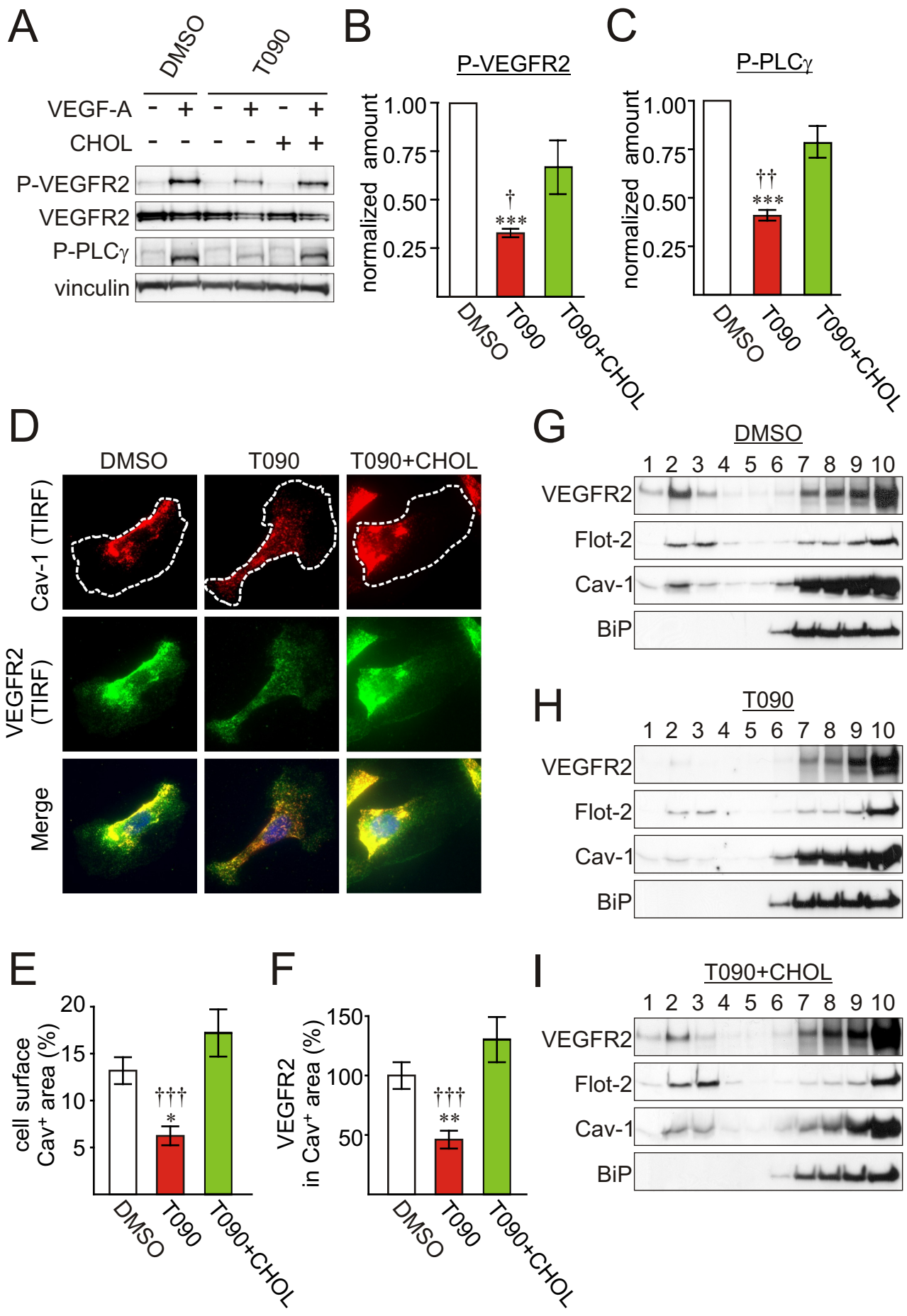

Figure 4

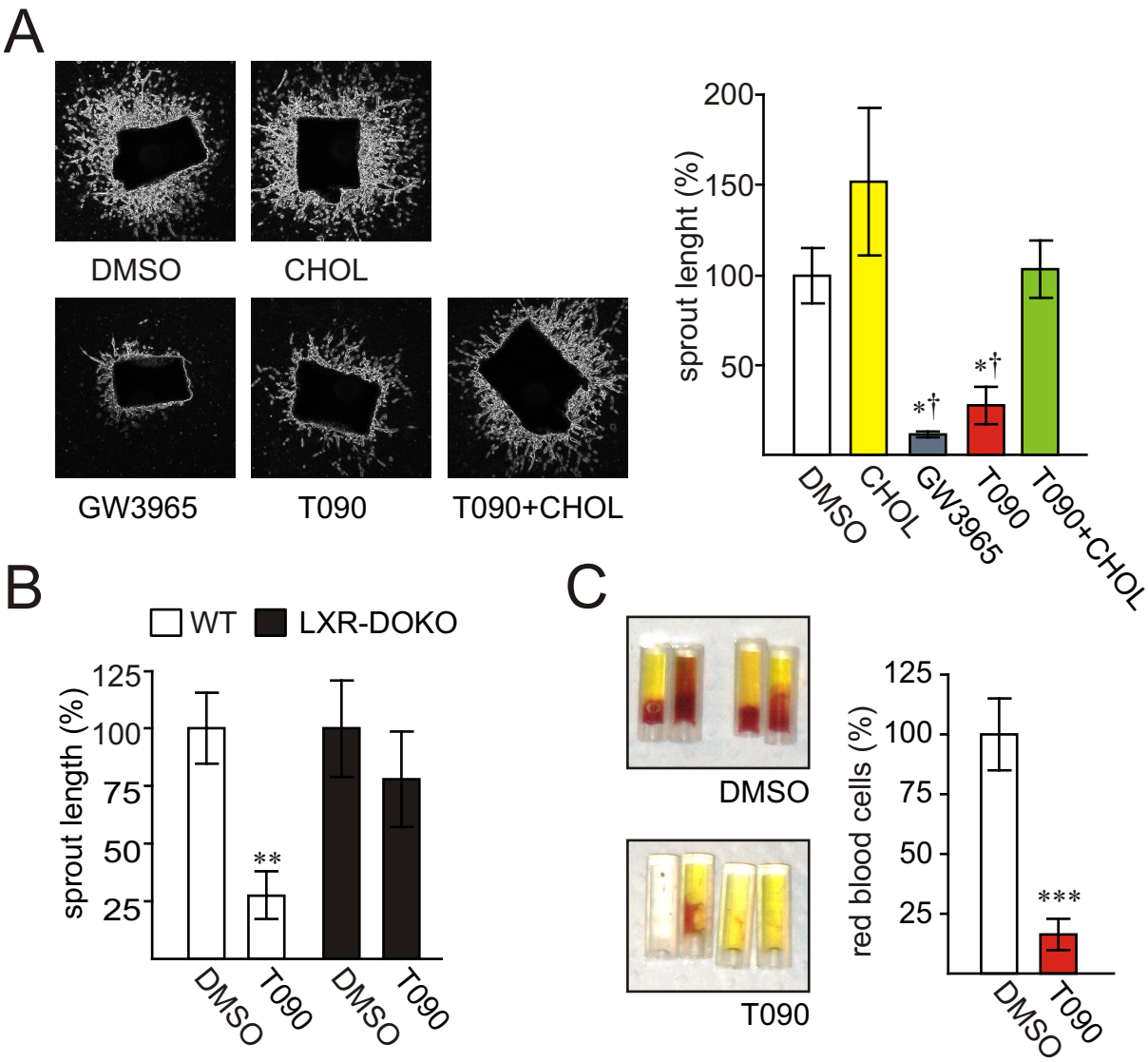

Figure 5

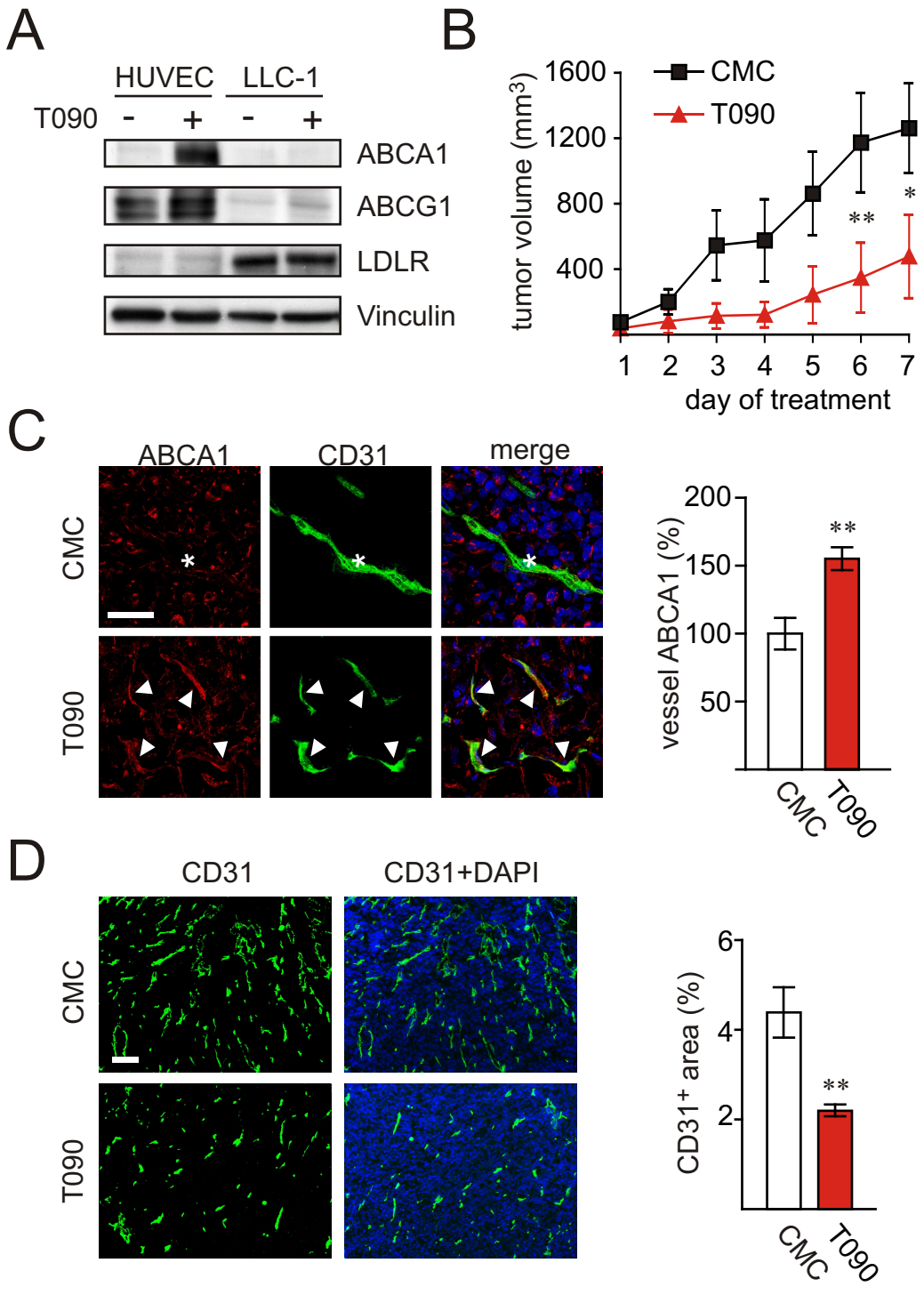

Figure 6

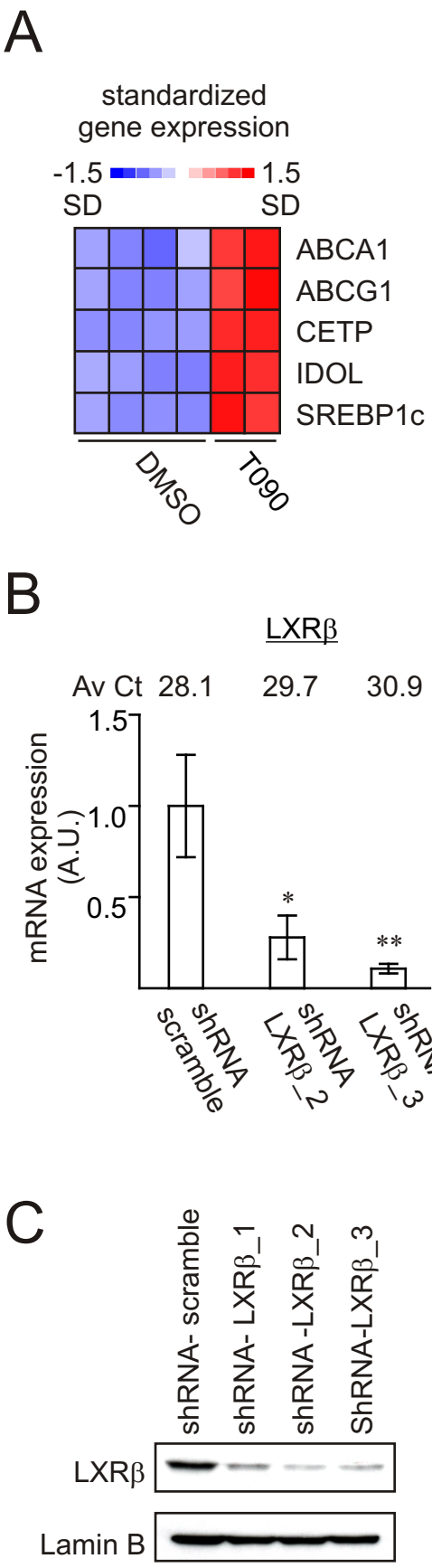

Supplementary Figure I

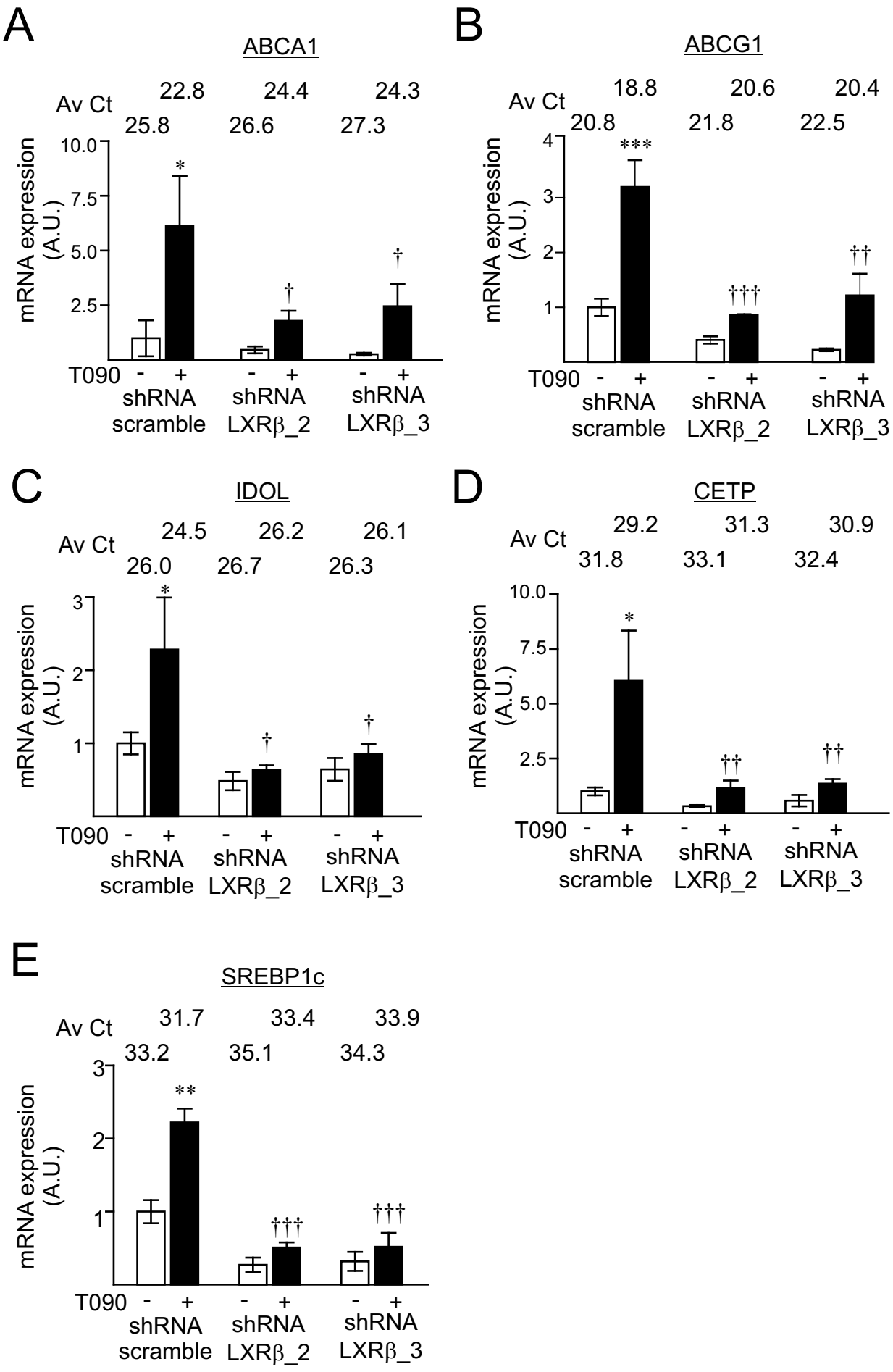

Supplementary Figure II

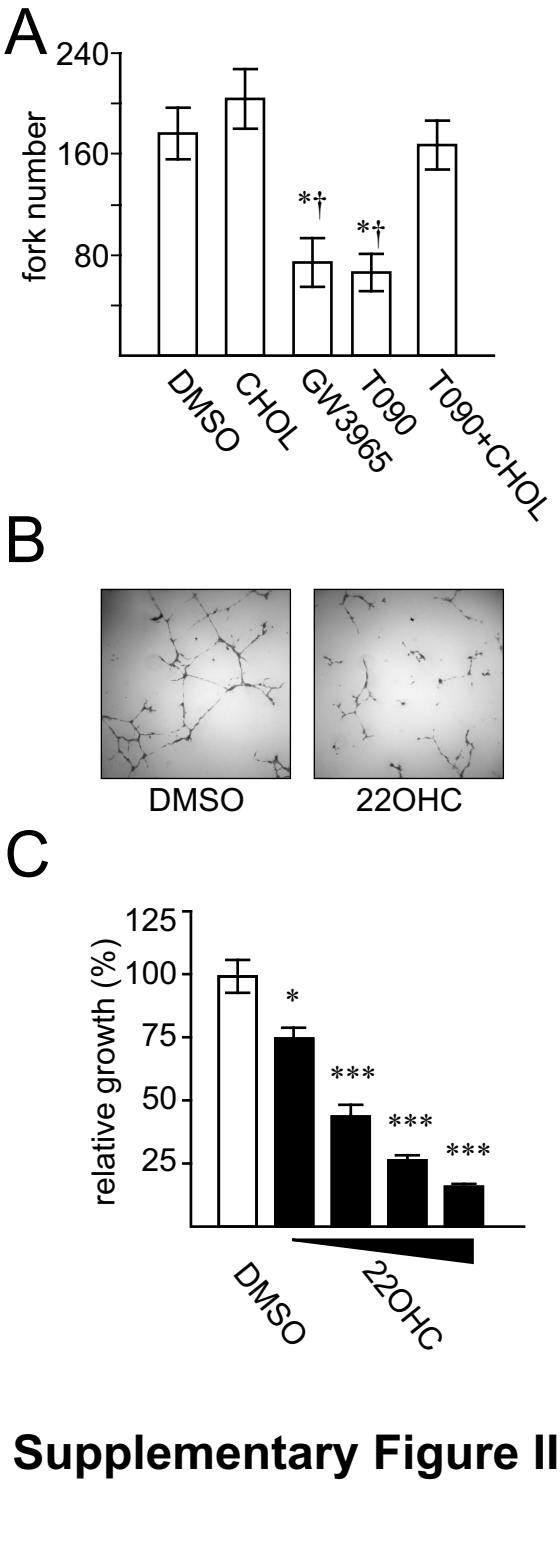

Supplementary Figure III

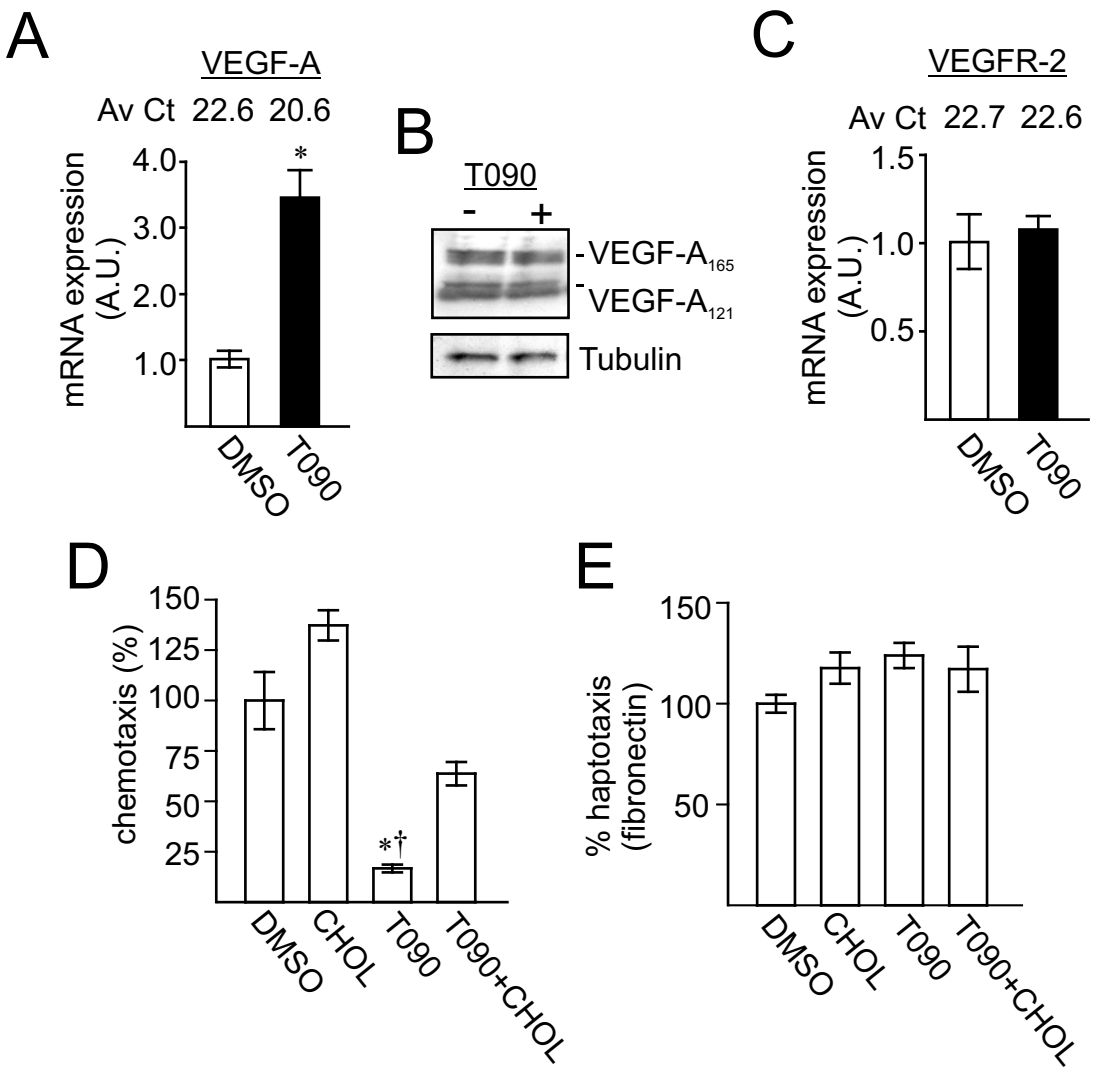

Supplementary Figure IV

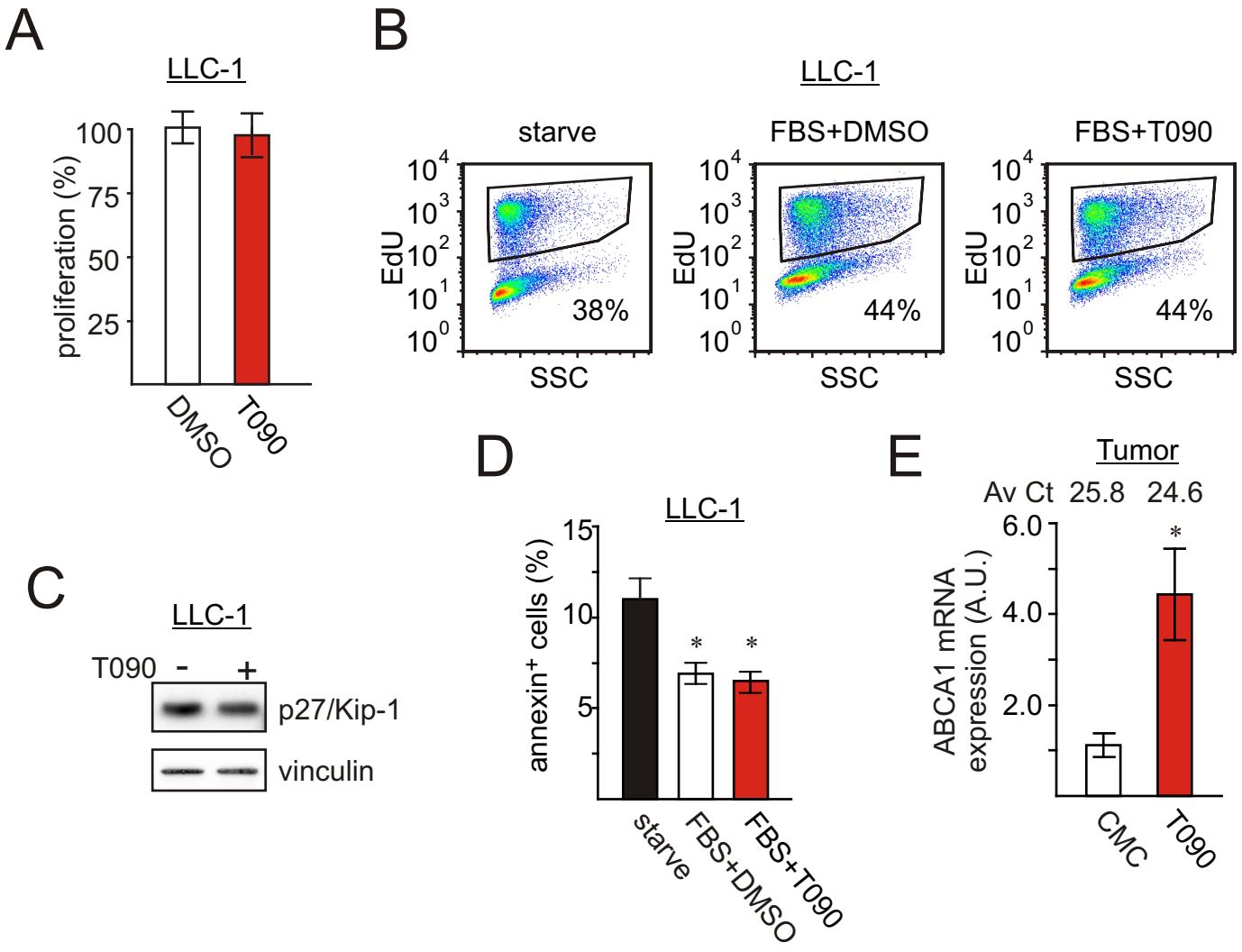

Supplementary Figure V